Grain boundary composition and conduction in HfO2: An ab initio study

K.-H. Xue, P. Blaise, L. R. C. Fonseca, G. Molas, E. Vianello et al.

Citation: Appl. Phys. Lett. **102**, 201908 (2013); doi: 10.1063/1.4807666
View online: http://dx.doi.org/10.1063/1.4807666
View Table of Contents: http://apl.aip.org/resource/1/APPLAB/v102/i20
Published by the American Institute of Physics.

Grain boundary composition and conduction in HfO_2: An *ab initio* study

K.-H. Xue,[1] P. Blaise,[2] L. R. C. Fonseca,[3] G. Molas,[2] E. Vianello,[2] B. Traoré,[2] B. De Salvo,[2] G. Ghibaudo,[1] and Y. Nishi[4]
[1]*IMEP-LAHC, Minatec-INPG, 3 rue Parvis Louis Néel, BP 257, 38016 Grenoble Cedex 1, France*
[2]*CEA, LETI, Minatec Campus, 17 rue des Martyrs, 38054 Grenoble Cedex 9, France*
[3]*Center for Semiconductor Devices, State University of Campinas, Campinas, SP, Brazil*
[4]*Department of Electrical Engineering, Stanford University, Stanford, California 94305, USA*

(Received 11 March 2013; accepted 8 May 2013; published online 24 May 2013)

We investigate the electronic properties of HfO_2 grain boundaries employing a simple Σ5 (310)/[001] grain boundary model based on the cubic phase. Our calculations show the emergence of unoccupied defect states 0.4 eV below the conduction band due to the under-coordination of certain Hf ions in the grain boundary. They also show that migration of metal interstitials such as Hf and Ti to the grain boundary is energetically favorable, turning the grain boundary region metallic. This scenario may create leakage paths in poly-crystalline HfO_2 or serve as the conduction mechanism in resistive random access memories. © *2013 AIP Publishing LLC*. [http://dx.doi.org/10.1063/1.4807666]

In microelectronics HfO_2 is the gate dielectric basic ingredient in state-of-the-art CMOS.[1] It is also a promising candidate material for resistive random access memories (RRAMs).[2] In both applications, unlike the corresponding SiO_2-based dielectrics, HfO_2 may become partly or entirely crystallized after the required thermal treatment.[3] The poly-crystalline nature of HfO_2 thin films brings about additional challenges associated with the grain boundary (GB). While in MOS applications certain doping schemes can be employed to keep HfO_2 amorphous,[4] poly-crystalline thin films are sometimes believed to be beneficial to RRAM applications. This is because soft breakdown may take place more easily along GBs than in the monoclinic HfO_2 (m-HfO_2) grains, due to either defect segregation or the thermal grooving effect,[5] lowering the operation voltages.[6]

While it is generally accepted that the GB region is a preferred leakage path in poly-HfO_2,[7] relatively few studies have been published where the conduction mechanism of an HfO_2 GB is investigated. McKenna *et al.*[8–11] employed *ab initio* calculations to estimate the formation energies and electronic structures of various m-HfO_2 GB models and concluded that the (101) twin boundary possesses the lowest formation energy. This GB is shown to be a possible percolation path for electron tunneling due to oxygen vacancy segregation.[8] Bersuker *et al.* calculated its density of states (DOS) considering a high concentration of oxygen vacancies, and showed a conductive sub-band within the original band gap.[11]

The study of GBs in zirconia, an isomorph of hafnia, has been focused on the cubic fluorite phase Y-stabilized zirconia (YSZ), which finds an important application as the electrolyte in fuel cells.[12] Previous works on YSZ GBs[13,14] explored some low-Σ coincidence site lattice[15] (CSL) tilt GBs (such as the Σ5 36.87° (310)/[001] GB), as well as some minor modifications of them.

Inspired by these studies, we have investigated defects in the CSL model of cubic fluorite HfO_2 and linked our results to possible conductive paths through GBs. Even though in HfO_2 the cubic phase at normal pressure is stable only at high temperature for bulk, in thin films it does emerge in some occasions.[16] However, the main benefit of such a simple model lies in the ease to clarify the most significant rules and phenomena. We expect that our findings are general enough to be relevant in experimental conditions.

In this study, we employed first principles density functional theory[17,18] (DFT) as implemented in the plane-wave based Vienna *Ab initio* Simulation Package[19,20] (VASP). We adopted projector augmented-wave pseudopotentials[21,22] including Hf 5*p*, 5*d*, and 6*s* electrons and O 2*s* and 2*p* electrons in the valence. The generalized gradient approximation (GGA) was used for the exchange-correlation energy within the Perdew-Burke-Ernzerhof functional.[23] A plane wave cut-off energy of 500 eV yields well-converged values. Sufficiently dense Γ-centered Monkhorst-Pack[24] k-meshes were utilized for sampling the Brillouin zone. The lattice constant of cubic HfO_2 was relaxed to 5.075 Å, which fits well the experimental value 5.08 Å.[25] The GB supercell was constructed by combining two grains with a tilt angle $2atan(1/3) = 36.87^{o}$ (see Fig. 1), where two boundaries of opposite directions occur alternately along the b direction (located at $y = 0$ and $y = 0.5$, respectively) in order to satisfy the periodic boundary conditions. The degree of site matching is characterized by Σ, where a low value indicates a high coincidence. In cubic systems, Σ is simply evaluated as[26]

$$\Sigma = \delta \times (h^2 + k^2 + l^2), \tag{1}$$

where (h, k, l) is the direction of the boundary in the coordinate system of one of the grains: $\delta = 1$ if $(h^2 + k^2 + l^2)$ is odd and $\delta = 1/2$ if $(h^2 + k^2 + l^2)$ is even. In the CSL model $h = 3$, $k = 1$, and $l = 0$, thus $\Sigma = 5$, indicating high symmetry and possibly low formation energy. The dimension of the supercell was fixed to 8.024 Å × 48.146 Å × 5.075 Å, which is the calculated size of the perfect GB geometry. The atomic coordinates were relaxed until all Hellmann-Feynman forces were less than 0.04 eV/Å. A similar model proposed by Kingery[27] (Fig. 1) was also constructed by removing one HfO_2 chemical unit per GB in the supercell. The total number of atoms per supercell is 180 and 174 for the CSL and the Kingery models, respectively.

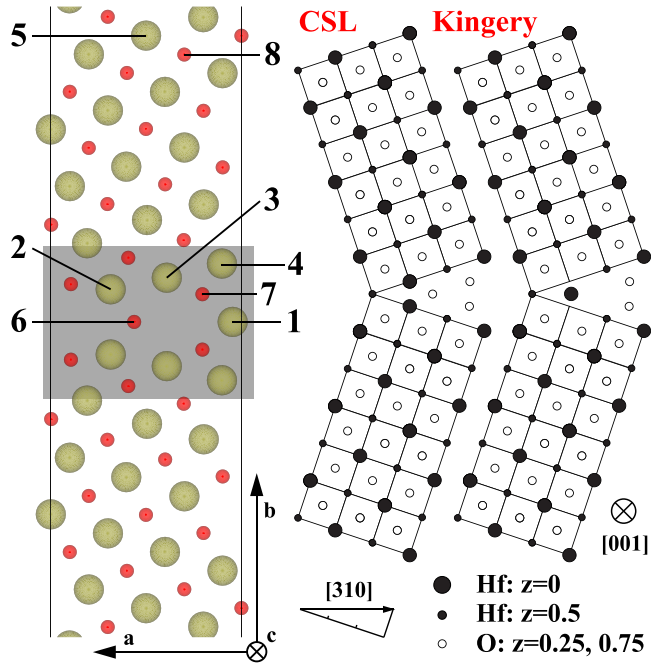

FIG. 1. (Left) Atomistic representation of the CSL grain boundary in cubic HfO_2, with atomic coordinates optimized and particular sites numbered. Big, green balls stand for hafnium while small, red balls stand for oxygen. The shaded square indicates the grain boundary region. (Right) Schematic non-optimized geometry of the Σ5 36.87° (310)/[001] CSL and Kingery grain boundary models. z = 0 is the topmost plane of atoms in the unit cell.

The formation enthalpy of a GB per unit area can be defined as the energy required to transform the same moles of single crystal material into poly-crystalline material. We have calculated the formation enthalpies for the CSL and Kingery models and found 2.92 J/m^2 and 3.14 J/m^2, respectively. Because the formation enthalpy of the CSL model is lower, we chose it as the focus of this paper. The DOS of the CSL model is shown in Fig. 2, where additional states emerge in the forbidden band near the band edges of bulk

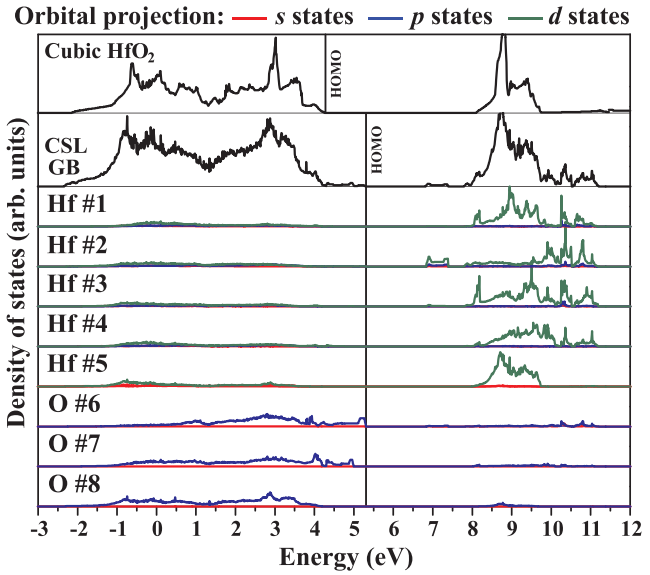

FIG. 2. Total DOS and site-projected partial DOS for the CSL grain boundary model. The DOS for single crystal cubic HfO_2 is shown for comparison. The highest occupied molecular orbitals (HOMOs) are indicated by vertical lines. Atom numbers follow the convention introduced in Fig. 1.

cubic hafnia. To identify the origin of these states, we plotted the site-projected DOS. As shown in Fig. 2, the GB states close to the conduction band (CB) originate from Hf atom #2 (see numbering convention in Fig. 1), which lies close to the center of the GB, lacking oxygen coordination. The energy gap between the 5*d*-like GB band and the CB is 0.4 eV. Similarly, the GB states close to the valence band (VB) stem from the O atoms #6 and #7 located in the GB in the Hf-poor environment. While the global stoichiometry of the CSL model is HfO_2, its tilt angle results in insufficient bonding for certain cations and anions in the GB region, leading to the extra band gap states. Our results are qualitatively consistent with the experimental data of Nguyen *et al.* who observed unoccupied defect states 0.2–0.3 eV below the CB in poly-crystalline hafnia.[28]

Seven variations of the CSL model are shown in Fig. 3 with their atomic coordinates optimized. They comprise three stoichiometric models, namely the CSL and the Kingery models, plus our new "compact" model (186 atoms, formation enthalpy 3.50 J/m^2) obtained through the addition of one HfO_2 chemical unit per GB in the CSL supercell (Figs. 3(a)–3(c)). There are also three defective non-stoichiometric intrinsic models (Figs. 3(d)–3(f)), and two defective stoichiometric extrinsic models (Figs. 3(g) and 3(h)). The defective intrinsic models (d)–(f) involve only atomic species present in hafnia, namely, Hf and O. With all defects placed in each GB, these defects are one or two O vacancies (Fig. 3(d)), one O interstitial (Fig. 3(e)), and one Hf interstitial (Fig. 3(f)). The defective extrinsic models contain atomic species not present in native hafnia, but common in metal electrodes from where they are believed to migrate to the dielectric. They are a Ti interstitial (Fig. 3(g)) representing reactive electrodes, and a Pt interstitial (Fig. 3(h)) representing inert electrodes. Both metal interstitials are located in the GB, with the concentration of one metal atom per GB.

The formation energy of a neutral defect X is defined as

$$E_{for} = E_D - E_0 \pm \mu_X, \tag{2}$$

where E_D is the energy of the defective supercell, E_0 is the energy of the defect-free supercell, and μ_X is the chemical potential of species X. The plus sign is for X vacancies while the minus sign is for X interstitials. We chose μ_O as half the chemical potential of an oxygen molecule, and μ_{Hf}, μ_{Ti}, and μ_{Pt} as the chemical potential of hcp Hf, hcp Ti, and fcc Pt, respectively. The formation energy of an oxygen vacancy in the GB region of the CSL model is 4.69 eV, more than 2 eV lower than in bulk (6.75 eV).[29] If the oxygen chemical potential is chosen as that of an oxygen interstitial in hcp Ti, this formation energy is further minimized to −1.55 eV,[30] which implies that oxygen vacancies may favorably emerge in the GB region when a reactive metal such as Ti is attached to the oxide. The formation energy of an oxygen interstitial in the GB region of the CSL model is slightly lower than in bulk (0.70 eV compared with 1.05 eV). For the metals considered, their incorporation energies in the CSL GB are −0.18 eV, −0.61 eV, and 3.64 eV for Hf, Ti, and Pt, respectively. The incorporation energies of Hf and Ti are considerably lower than in bulk cubic HfO_2, i.e., 4.03 eV and 2.40 eV, respectively, indicating that the accumulation of

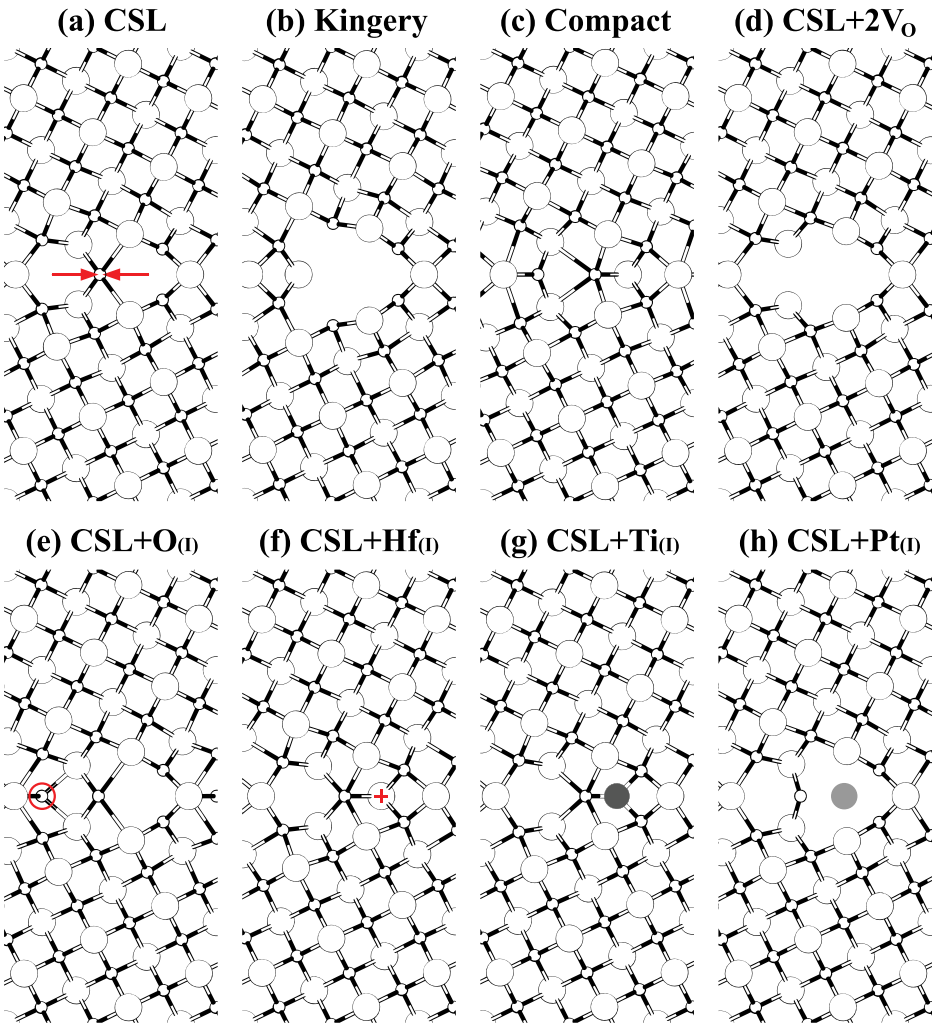

FIG. 3. *c*-direction view of various grain boundary models with their atomic positions optimized. Big (small) hollow balls stand for hafnium (oxygen). In (a) the two arrows indicate the two O atoms (the lower one is hidden by the upper one in this perspective) removed to generate the configuration shown in (d); in (e) and (f) the circle and the cross indicate the locations of the O and Hf interstitials, respectively; in (g) and (h) foreign interstitial Ti and Pt atoms, respectively, are represented by solid balls.

these species in the GB is favored with respect to the grains. Moreover, the negative formation energy for Ti reveals that its migration from the metal electrodes to the GB is energetically favorable.

Figures 4(a)–4(c) show that the DOS of the CSL, Kingery, and compact models retain the basic features of the DOS of cubic hafnia, but with long tails above the VB and below the CB edges for the CSL model, mostly a long tail below the CB for the Kingery model, and short tails above the VB and below the CB for the compact model. The Kingery model has more GB states below the CB than the CSL model due to the presence of more under-bonded Hf cations, while the compact model shows almost no gap states because both cations and anions are better saturated in the GB region. The introduction of one oxygen vacancy in the GB only leads to a deep fully occupied band (indicated by #1 in Fig. 4(d)) in the band gap, which does not support metallic conduction through the GB region. To test this idea further, we added one more oxygen vacancy per GB. Even though the formation energy per oxygen vacancy in this case (5.46 eV) is again lower than in bulk, the extra fully occupied band in the band gap (indicated by #2 in Fig. 4(d)) still falls short of closing the energy gap (Fig. 4(d)). The introduction of an oxygen interstitial near atom Hf #2 has the effect of suppressing some of the gap states near the band edges of the CSL model, mostly those near the CB edge, as shown in Fig. 4(e). On the other hand, Figs. 4(f) and 4(g) show that Hf and Ti interstitials in the GB yield metallic states, while the Pt interstitial in the GB does not.

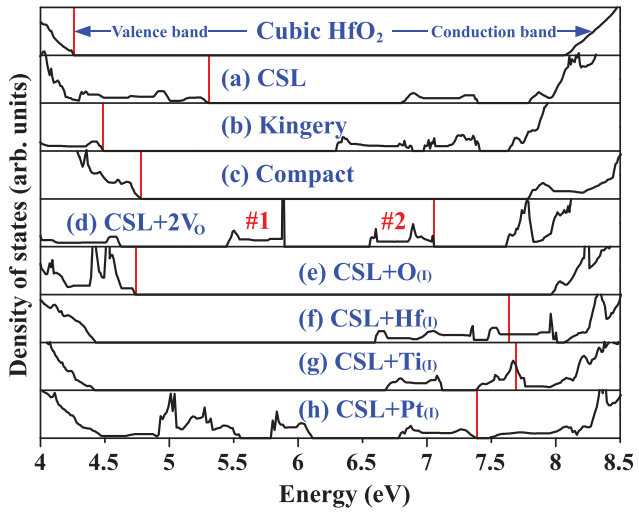

FIG. 4. DOS for the models shown in Fig. 3. In (d), the band marked by #1 is created by one O vacancy per GB, while two vacancies per GB result in the two bands marked by #1 and #2. Vertical red lines indicate the Fermi level [for (f) and (g)] or HOMO (for the rest).

The metallic band structure calculated for metal-doped GB is not evident since the metal ions in the GB environment form bond to their oxygen neighbors, possibly resulting in a metal-oxide that in general is not a metal. To shed some

light on the conductivity induced by Hf or Ti interstitials in the GB (and the lack of conductivity in the Pt case), we have estimated the amount of charge exchanged between the metal cations and the surrounding oxygen anions through Bader analysis. The calculated charges of the Hf and Ti interstitials are +2.01 e and +1.70 e, respectively. In contrast, the charge of an Hf cation in bulk cubic HfO_2 is +2.72 e, while the charge of a Ti cation in bulk rutile TiO_2 is +2.31 e. The lower Hf ion charges may stem from its lower coordination to oxygen in the GB: the Hf ion is 6-fold coordinated in the GB but 8-fold coordinated in bulk. Differently, the Ti ion is 6-fold coordinated both in the GB and in bulk. However, the average Ti–O bond length for the Ti interstitial in the GB (2.04 Å) is larger than in bulk rutile TiO_2 (1.98 Å). Longer bonds are generally associated with less charge exchange. In both cases, the lower valence of the metal ions associated with conduction is consistent with the GB reduction scenario envisaged by Gilmer *et al.*[7] Interestingly, in the recently predicted semi-metallic Hf_2O_3 phase the Bader charge of Hf is +2.10 e,[30] close to +2.01 e found in this work for the Hf interstitial in the GB. The Bader charge of the Pt interstitial in the GB is rather small, −0.14 e, which reflects the inert characteristic of this atom.

In conclusion, we have shown that a CSL GB model of cubic HfO_2 displays states in the band gap originating from under-coordinated Hf or O ions in the GB region, even if the material as a whole is stoichiometric. Such under-bonding in the GB may explain the unoccupied defect states below the conduction band observed experimentally in poly-crystalline HfO_2.[28] In addition, the formation energies for both oxygen vacancies and metal or oxygen interstitials are lower in the GB than in bulk cubic HfO_2. Moreover, we have found that in the presence of a Ti electrode it is energetically favorable for oxygen to migrate from the GB to the electrode, leaving the GB oxygen-poor. The formation energies of the metal atoms Hf and Ti considered in this work, placed in interstitial positions of the GB, are also negative with respect to their metal phase, favoring their migration from the electrodes or from metal-rich clusters to the GB. The accumulation of metal atoms in the GB may render it metallic, offering a conduction path between the electrodes. Therefore, the GB facilitates both the formation of oxygen vacancies and the incorporation of reactive metals in the oxide. Our GB model indicates that through metal doping the GB becomes metallic, thus offering a possible explanation for the ON-state of HfO_2 RRAM.

We thank C. Guedj from CEA-LETI for experimental data on hafnia grain boundary and helpful discussions. This work was financially supported by the Nanosciences Foundation of Grenoble, France. LRCF also thanks INCT/Namitec and CNPq for financial support. The calculations were performed on the Stanford NNIN Computing Facility funded by the National Science Foundation of USA.

[1]J. Kavalieros, B. Doyle, S. Datta, G. Dewey, M. Doczy, B. Jin, D. Lionberger, M. Metz, W. Rachmady, M. Radosavljevic *et al.*, Dig. Tech. Pap. - Symp. VLSI Technol. **2006**, 50.
[2]K.-L. Lin, T.-H. Hou, J. Shieh, J.-H. Lin, C.-T. Chou, and Y.-J. Lee, J. Appl. Phys. **109**, 084104 (2011).
[3]E. P. Gusev, C. Cabral, Jr., M. Copel, C. D'Emic, and M. Gribelyuk, Microelectron. Eng. **69**, 145 (2003).
[4]S. V. Ushakov, C. E. Brown, and A. Navrotsky, J. Mater. Res. **19**, 693 (2004).
[5]W. W. Mullins, J. Appl. Phys. **28**, 333 (1957).
[6]M. Lanza, K. Zhang, M. Porti, M. Nafría, Z. Y. Shen, L. F. Liu, J. F. Kang, D. Gilmer, and G. Bersuker, Appl. Phys. Lett. **100**, 123508 (2012).
[7]D. C. Gilmer, R. Hegde, R. Cotton, R. Garcia, V. Dhandapani, D. Triyoso, D. Roan, A. Franke, R. Rai, L. Prabhu *et al.*, Appl. Phys. Lett. **81**, 1288 (2002).
[8]K. McKenna and A. Shluger, Appl. Phys. Lett. **95**, 222111 (2009).
[9]K. P. McKenna and A. L. Shluger, Microelectron. Eng. **86**, 1751 (2009).
[10]K. McKenna, A. Shluger, V. Iglesias, M. Porti, M. Nafría, M. Lanza, and G. Bersuker, Microelectron. Eng. **88**, 1272 (2011).
[11]G. Bersuker, D. C. Gilmer, D. Veksler, P. Kirsch, L. Vandelli, A. Padovani, L. Larcher, K. McKenna, A. Shluger, V. Iglesias *et al.*, J. Appl. Phys. **110**, 124518 (2011).
[12]S. C. Singhal, Solid State Ionics **135**, 305 (2000).
[13]C. A. J. Fisher and H. Matsubara, J. Eur. Ceram. Soc. **19**, 703 (1999).
[14]E. C. Dickey, X. Fan, and S. J. Pennycook, J. Am. Ceram. Soc. **84**, 1361 (2001).
[15]M. L. Kronberg and F. H. Wilson, Trans. AIME **185**, 501 (1949).
[16]C. Zhao, V. Cosnier, P. J. Chen, O. Richard, G. Roebben, J. Maes, S. Van Elshocht, H. Bender, E. Young, O. Van der Biest *et al.*, Mater. Res. Soc. Symp. Proc. **745**, N1.5 (2002).
[17]P. Hohenberg and W. Kohn, Phys. Rev. **136**, B864 (1964).
[18]W. Kohn and L. J. Sham, Phys. Rev. **140**, A1133 (1965).
[19]G. Kresse and J. Furthmüller, Comput. Mater. Sci. **6**, 15 (1996).
[20]G. Kresse and J. Furthmüller, Phys. Rev. B **54**, 11169 (1996).
[21]P. E. Blöchl, Phys. Rev. B **50**, 17953 (1994).
[22]G. Kresse and D. Joubert, Phys. Rev. B **59**, 1758 (1999).
[23]J. P. Perdew, K. Burke, and M. Ernzerhof, Phys. Rev. Lett. **77**, 3865 (1996).
[24]H. J. Monkhorst and J. D. Pack, Phys. Rev. B **13**, 5188 (1976).
[25]I. A. El-Shanshoury, V. A. Rudenko, and I. A. Ibrahim, J. Am. Ceram. Soc. **53**, 264 (1970).
[26]P. Lejček, *Grain Boundary Segregation in Metals* (Springer, Berlin, Germany, 2010).
[27]W. D. Kingery, J. Am. Ceram. Soc. **57**, 1 (1974).
[28]N. V. Nguyen, A. V. Davydov, D. Chandler-Horowitz, and M. M. Frank, Appl. Phys. Lett. **87**, 192903 (2005).
[29]To calculate the energy of the oxygen molecule, we implemented the 1.36 eV energy adjustment proposed by Wang *et al.* to correct a well-known DFT/GGA error: L. Wang, T. Maxisch, and G. Ceder, Phys. Rev. B **73**, 195107 (2006).
[30]K.-H. Xue, P. Blaise, L. R. C. Fonseca, and Y. Nishi, Phys. Rev. Lett. **110**, 065502 (2013).